ELSEVIER

Journal of Hazardous Materials 142 (2007) 324–331

Journal of Hazardous Materials

www.elsevier.com/locate/jhazmat

Filtration of dust in a circulating granular bed filter with conical louver plates (CGBF-CLPs)

Jing-Cheng Bai [a], Shu-Yii Wu [a,b,*], An-Sheng Lee [a], Chen-Yeon Chu [b]

[a] *Department of Chemical Engineering, Feng Chia University, Taiwan, ROC*
[b] *Research Center for Energy & Resources, Feng Chia University, Taiwan, ROC*

Received 23 May 2006; received in revised form 11 August 2006; accepted 11 August 2006
Available online 18 August 2006

Abstract

A novel circulating granular bed filter with conical louver plates (CGBF-CLPs) was designed to remove dust particulates from the flue gas stream of a coal power plant. The purpose of this investigation was to evaluate the performance of the CGBF-CLPs. Dust collection efficiency and pressure drop data were analyzed to determine better operating conditions. The effect of solid mass flow rate, collector particle size and dust/collector particles separator types on the dust collection efficiency and pressure drop in the CGBF-CLPs were investigated in this study. The solid mass flow rate (B) varied from 15.59 ± 0.44 to $20.36 \pm 0.68\ g\ s^{-1}$ and the initial average collector particle sizes were 1500 and 795 μm, respectively. Two types of separators, a cyclone and an inertial one, for separating the dust and collector particles were used in the CGBF-CLPs system. An Air Personal Sampler (SKC PCXR8) was used to determine the inlet and outlet dust concentrations. A differential pressure transmitter and data acquisition system were used to measure the pressure drop. Experimental results showed that the highest dust collection efficiency was 99.59% when the solid mass flow rate was $17.08 \pm 0.48\ g\ s^{-1}$ and the initial average collector particle size was 795 μm with the cyclone type separator. The results showed that the attrition fines of the original collector particles returning to the granular bed filter (GBF) reduced bed voidage. This phenomenon significantly increased the dust collection efficiency in the CGBF-CLPs. As a consequence, a bigger bed voidage creates a lower dust collection efficiency in the GBF.

Keywords: Conical louver plates; Granular bed filter; Dust collection efficiency; Pressure drop

1. Introduction

Evaluating the performance of the circulating granular bed filter with conical louver plates (CGBF-CLPs) designed for flue gas clean up is the primary purpose of this research paper. Particulate matter must be removed from flue gas because of the particulate emission limit requirement of gas turbine. A typical circulating granular bed filter (CGBF) can be set up for the integrated gasification combined cycle (IGCC) process for flue gas cleaning [1]. Pressurized-fluidized bed combustion (PFBC) technology and IGCC systems are notable for power generation through the expansion of high-pressure and high-temperature flue gas turbines. In these processes, the flue gas or exhaust gas stream carries high concentrations of dust. The dust must be removed to increase the life of the gas turbine [2,3]. The granular bed filter, by employing low cost refractory granular as better material, makes it a better alternative for high temperature and pressure gas cleaning [4]. The flow patterns and velocity fields of GBF in a moving bed with various louver angles have been investigated [1]. A proper configuration of the louver angle can prevent a dead zone from forming in the plate of the filter.

Dust collection efficiency of a moving granular bed filter is a function of solids mass flow rate, particle size, superficial gas velocity and the properties of the flue gas and dust [5,6]. Various mechanisms can act in the dust filtration process. They cause deposition of dust particles upon an area of collectors in the space of a granular bed void system. Brown et al. [7] found that the thickness of dust cake can be controlled to give high dust collection efficiency and acceptable pressure drop by changing

Abbreviations: CGBF, circulating granular bed filter; CLPs, conical louver plates; GBF, granular bed filter; IGCC, integrated gasification combined cycle; MCE, mixed cellulose esters; PFBC, pressurized-fluidized bed combustion

* Corresponding author at: Department of Chemical Engineering, Feng Chia University, P.O. Box 25-102, Taichung 407, Taiwan, ROC. Tel.: +886 4 24517250x3679; fax: +886 4 24510890.
E-mail address: sywu@fcu.edu.tw (S.-Y. Wu).

0304-3894/$ – see front matter © 2006 Elsevier B.V. All rights reserved.
doi:10.1016/j.jhazmat.2006.08.026

Nomenclature

B	solids mass flow rate (kg s^{-1})
C_{in}	inlet dust concentration (ppmw)
C_{out}	outlet dust concentration (ppmw)
d	conical louver spacing (cm)
d_p	average collector particle size (μm)
d_{p0}	initial average collector particle size (μm)
d_{100}	particle diameter at collector efficiency 100% (μm)
d_{sv}	surface/volume diameter (μm)
D_B	the diameter of the conical louver plate at the bottom (cm)
D_L	the diameter of the conical louver plate at the top (cm)
F	the percentage of attrition fines (%)
H	granular bed height (cm)
H_L	conical louver plate height (cm)
ppmw	parts per million by weight
P_f	particle size distribution of the finial collector particles (μm)
P_0	particle size distribution of the initial collector particles (μm)
ΔP	pressure drop (kPa)
Q_0	injection gas-volumetric flow rate (m^3 s^{-1})
t	collection time of the collector particles (min)
U_{mf}	minimum fluidized velocity (m s^{-1})
U_t	terminal velocity (m s^{-1})
W	accumulation weight of collector particles (kg)

Greek letters

η	dust collection efficiency (%)
θ	conical louver angle (°)
ρ	particle density (kg cm^{-3})

the flow rate of granular media. The granular filters often have a layer structure with decreasing collector particle size in the flow direction and the granular layer removes aerosol particles of decreasing size [8]. Jordan et al. [9] stated that a good granular bed filter could be characterized by low pressure drop, high dust collection efficiency and high capacity (operating for along time without shutdown). For the successful operation of a granular bed filter, the pressure drop signal can let the operator understand filtration conditions and determine the main factor affecting dust collection efficiency.

Miyamoto and Bohn [10] found that the pressure drop through the gravel layer was discernible when the granular reached a threshold load but the pressure drop increased abruptly with erratic fluctuations. Tsubaki and Tien [11] investigated gas filtration in a cross flow moving granular bed filter. When the gas velocity was lower than 0.05 m s^{-1}, the pressure drop was independent of time and solid velocity. Jordan and Linder [12] developed and studied multilayer sand granular bed filters. There was a mechanism explaining clogging caused by pressure drop and the penetration of sand granular bed filters. As a filter removes dust particles from a gas stream, the initial pressure drop across the filter increases [13].

The CGBF-CLPs is a continuously moving granular bed filter that consists of a cylinder column in this investigation. The primary advantages of CGBF-CLPs are continuous operation without closing down for back washing and reduce the volume of setup. The CGBF-CLPs was setup using three parts, a granular bed filter, a riser and a dust/collector particles separator in the inlet of the GBF. The riser was designed for the transport of collector particles to the dust/collector particles separator. The separator was designed for dust/collector particles separation to get refreshing collector particles and allow the granular bed filter to operate continuously.

In this investigation, the dust collection efficiency and pressure drop were analyzed to find suitable operating conditions and determine the effects of solids mass flow rate, collector particle size and the separator type.

2. Experimental apparatus and procedures

The experimental apparatus in this study consisted of the CGBF-CLPs system, the dust gas-generating system and the sampling system. A schematic diagram of the experimental apparatus used in this study is shown in Fig. 1.

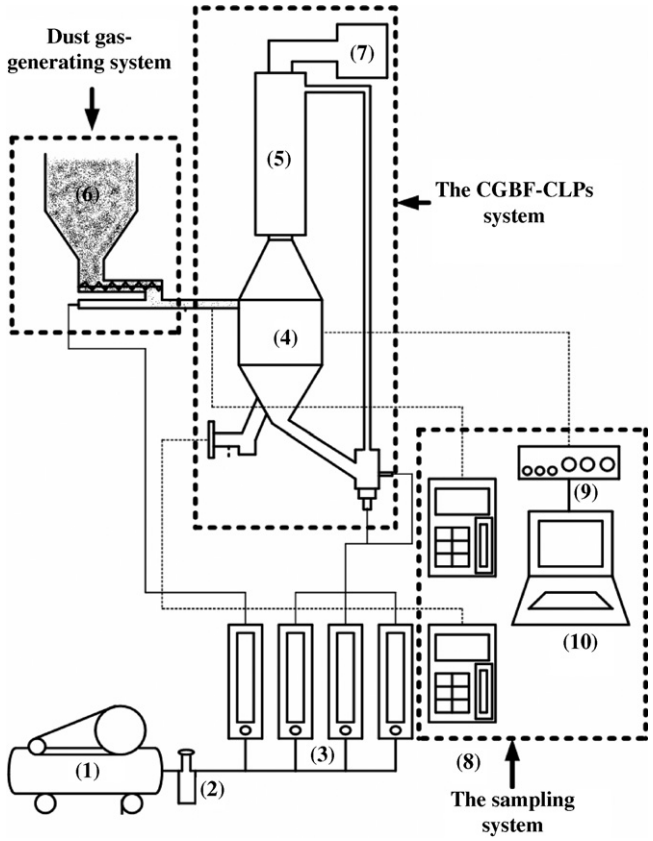

Fig. 1. Schematic diagram of the experimental apparatus, where (1) air compressor, (2) pressure regulator, (3) rotameters, (4) CGBF-CLPs, (5) gas–solid separator, (6) dust gas-generating system, (7) bag filter, (8) air sampling pump, (9) 750 interfaces of pressure sensor-differential and (10) personal computer (PC).

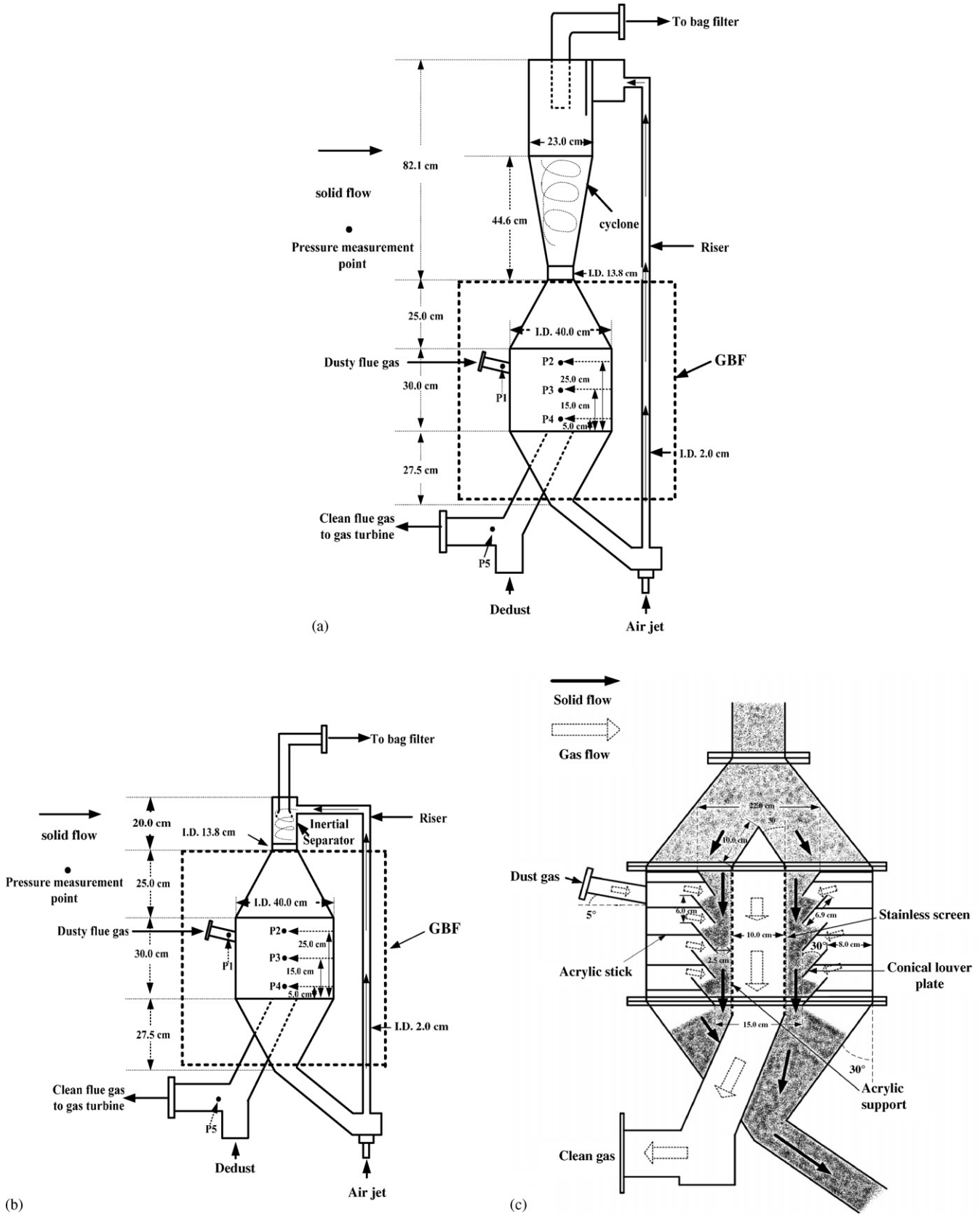

Fig. 2. The experimental rigs of the CGBF-CLPs system, where (a) cyclone type, (b) inertial separator type and (c) the conical louver plates in the GBF.

2.1. The CGBF-CLPs system

The experimental rig of the CGBF-CLPs system was setup in three parts, a GBF, a riser and a separator of dust and collector particles at the top of the GBF, as shown in Fig. 2. The GBF is a continuously moving granular bed filter and its advantageous feature is to prevent back washing without closing down. A dust separator and return loop were applied to catch collector particles leaving the riser. In order to easily observe the moving particles, the system was made by transparent acrylic plastic. The inner diameter and the height of the GBF were 40.0 and 82.5 cm, respectively. Moreover, the bottom of the riser was equipped with an air jet. The top of the GBF was an inversely conical hopper that was used to collect the collector particles from the separator. The height, inner diameters of the top and bottom of the inversely conical hopper were 25.0, 13.8 and 40.0 cm, respectively.

A separator was used to collect the recycled collector particles from the riser part in this system. The separators were designed for cyclone (Fig. 2(a)) and inertial separator (Fig. 2(b)). Fig. 2(a) indicated the scale of the cyclone type, the total height, the inner diameter, the inner diameter of the end of conical section and the height of the conical sections were 82.1, 23.0, 13.8 and 44.6 cm, respectively. The height and the inner diameter of the riser in the cyclone type were 189.0 and 2.0 cm, respectively. In addition, the height and the inner diameter of the inertial separator were 20.0 and 13.8 cm, respectively (Fig. 2(b)). The individual height and the inner diameter of the riser in the inertial separator type were 127.0 and 2.0 cm, respectively.

The GBF consisted of a thin bed of the collector particle held between these louver plates and a stainless screen (60 mesh). As shown in Fig. 2(c), there were five louver plates in the granular bed filter and the louver angle was built at 30°. The flowing property of collector particle depends on the angle of repose and the angle was usually lower than 60°. Bai et al. [1] found that a louver angle of 30° was the optimal dust collection point of efficiency. Therefore, the louver angle of the plate was set at 30° for this granular bed filter. The gas passed horizontally through the collector particles and moved downwards in the granular bed filter. A vertical layer of collector particles was supported by conical louver plates in the GBF.

2.2. Dust gas-generating system

A dust gas-generator was used to prepare the test dust gas at room temperature. The gas flow containing dust particles was provided by a screw feeder. The screw feeder was located at the inlet of the GBF. The dust particulate was injected by high pressure dry-air with a compressor. Before the dust particulate was packed up in the particulate hopper, it was dried at a low temperature to avoid bridge formation. The length, width and height of a particulate hopper were 20.0, 15.0 and 30.0 cm, respectively. For commercial scale applications and understanding the limitations of system filtration, the dust gas-generating system was operated with the inlet having a high dust average concentration of 27,513 ppmw. The dust concentration was controlled by the screw velocity. The dust particulate was transported to the granular bed filter by air injection. The injection gas-volumetric flow rate was 0.0133 $m^3\ s^{-1}$ at room temperature. The inner diameter and the length of the screw were 0.5 and 30.0 cm, respectively. The injection dust flow rate was 439.11 $mg\ s^{-1}$.

2.3. Sampling system

The outlet and inlet dust concentrations were determined by the weight of dust which was isokinetic collected by an Air Personal Sampler (SKC PCXR8). Eq. (1) is the expression of the dust collection efficiency (η). It is usually expressed as the performance of a GBF [14]

$$\eta\,(\%) = [1 - (C_{out}/C_{in})] \times 100 \quad (1)$$

where η is the dust collection efficiency, C_{out} is the outlet dust concentration and C_{in} is the inlet dust concentration. The dust collection efficiency (η) is the weight ratio of the dust collected to the dust entering the filter.

The sampling rate was 3.3 $L\ min^{-1}$ with the requirements of isokinetic sampling at the inlet slip stream and the sampling rate was 2.0 $L\ min^{-1}$ at the outlet slip stream. The sampling tube was made of stainless steel and the inner diameter was 5.0 mm. A sampling filter holder that housed a mixed cellulose esters (MCE) filter paper was connected to the sampling tube to capture dust. The sampling filter holder was renewed every 10 min. The filters containing dust were weighed and compared with the weight of filters before sampling. For sampler apparatus, the MCE filter paper diameter and aperture size were 37.0 mm and 0.45 μm, respectively. The MCE filter paper must be dried until the weight of the filter paper is constant. Finally, the dust captured in the sampling holder filter was scraped and analyzed to study the variation in the dust collection efficiency of the granular bed filter at the inlet and outlet of the granular bed filter.

2.4. The measurement of solids mass flow rate and pressure drop

To control the solids mass flow rates, a jet was set up at the bottom of the riser. The collector particles were collected at the top of the riser during a fixed time interval (t). The accumulating weight of collector particles (W) was then measured by weighing all the collected particles with an electronic balance. In order to reduce possible errors, more than 10 measurements were made under each operating condition. The average value of W was then used in Eq. (2) to obtain the solids mass flow rate (B)

$$B = W/t \quad (2)$$

where B is the solids mass flow rate, W is the accumulating weight of collector particles and t is the collection time of the collector particles.

The gas-volumetric flow rate versus solids mass flow rate with different average collector particle size are shown in Fig. 3. As shown in this figure, we found that the solids mass flow rate could be controlled by the operation of the gas-volumetric flow rate at the riser. The ranges of the solid mass flow rates are 15.59 ± 0.44

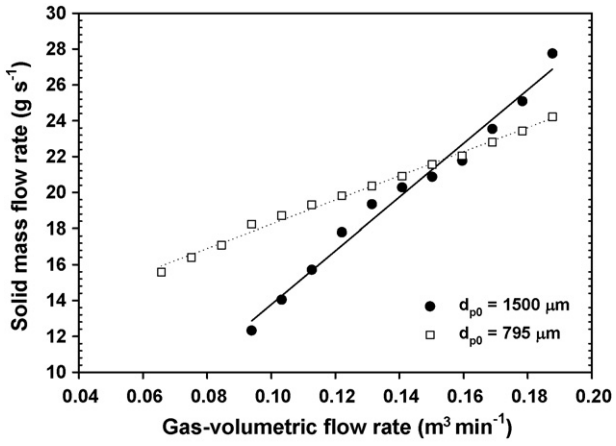

Fig. 3. The solids mass flow rate vs. gas-volumetric flow rate with different collector particle sizes.

to 20.36 ± 0.68 and 15.71 ± 0.59 to $20.28 \pm 0.24\,g\,s^{-1}$ with the initial average collector particle size of 795 and 1500 μm, respectively.

A differential pressure transmitter (PASCO-CI6533), high performance data acquisition card (PASCO-Science Workshop 750 Interface) and data treatment software (PASCO-Data Studio) were used to transform the analog signal of pressure drop into digital data. The pressure fluctuation data of points 1–5 was obtained by the pressure fluctuation diagram of the granular bed filter at different operating times with respect to the maximum pressure, minimum pressure and pressure sequence. A computer program used a method of statistics to calculate the outcome of the mean value and the standard deviation. There were five pressure measurement points in the CGBF-CLPs (Fig. 2). The pressure data of points 2, 3 and 4 were measured at a height of 25.0, 15.0 and 5.0 cm above the bottom of the GBF, respectively. The pressure data of points 1 and 5 were individually measured at the inlet of the dust gas and outlet of the clean flue gas of the GBF.

2.5. Materials

Silica sand was used as the collector particles in the GBF. The dust used in this study was taken from an electrostatic precipitator of a co-generation plant at the Chang Chun Company, Miao-Li, Taiwan. The main chemical compositions of the dust are SiO_2, Al_2O_3, CaO and Fe_2O_3. The particle size distribution and the surface/volumetric diameter (d_{sv}) of dust was measured by a laser particle size analyzer (FRITSCH-Analysette 22 Compact). The distribution range of dust particle size was 0.3–50 μm. The typical dust particle size distribution in this study is shown in Fig. 4. The initial weight of the collector particles was 45,000 g in the GBF. Two ranges of the initial collector particle sizes in the GBF were 2000–1000 and 1000–590 μm and the initial average collector particle sizes were 1500 and 795 μm, respectively.

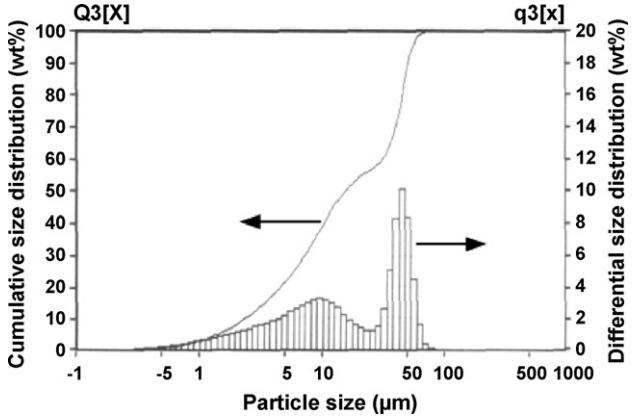

Fig. 4. The particle size distribution of the original dust.

Table 1
Properties of collector particles

Properties	Data
Minimum fluidized velocity, U_{mf} [21] ($cm\,s^{-1}$)	81.9/39.5
Geldart classification [18]	*B*
Particle density, ρ ($g\,cm^{-3}$)	2.58 ± 0.12
Ranges of the collector particle sizes (μm)	2000–1000/1000–590
Initial average collector particle sizes, d_{p0} (μm)	1500/795
Terminal velocity, U_t [22] ($cm\,s^{-1}$)	254.1/118.0

The densities of collector particles and dust were 2.58 ± 0.12, and $2.13 \pm 0.06\,g\,cm^{-3}$, which were measured by a particle density tester (TSUTSUI). The properties of collector particles are shown in Table 1.

2.6. Experimental procedures

Prior to each filtration experiment, we first packed up new collector particles of 45,000 g. Second, we opened the air compressor and refrigerated air dryer series. At the same time, the jet of the riser was operated to transport the collector particles and control the solids mass flow rates by an air rotameter. Third, the dust generator was started and allowed to run at the gas-volumetric flow rate of $0.0133\,m^3\,s^{-1}$. The dust was then allowed into the inlet of the granular bed filter and the dust gas was passed through the GBF after 10 min. Dust samples were taken isokinetically and simultaneously at both the inlet and the outlet of the granular bed filter at a constant gas flow rate. The samples were taken every 10 min and each experiment lasted for 50 min. At the same time, the pressure fluctuation was measured at each pressure measurement point. Finally, the dust collection efficiency data of the GBF was analyzed. Different operating conditions were adjusted for the next run. The experimental conditions were summarized in Table 2.

3. Results and discussion

3.1. Attrition phenomena and particle size distribution

The CGBF-CLPs used a riser of high gas velocity to transport the collector particles to the dust/collector particle separator. At the same time, high velocity gas resulted in an increase of the attrition of collector particles. In order to confirm the experiments were at a steady-state, the attrition experiments were carried out according to the percentage of attrition fines (*F*) with

Table 2
Experimental conditions in this study

Experimental parameters	Range
Inertial average collector particle sizes, d_{p0} (μm)	1500/795
Conical louver angle, θ (°)	30°
The diameter of conical louver plate at the top, D_L (cm)	22.0
The diameter of conical louver plate at the bottom, D_B (cm)	15.0
Conical louver spacing, d (cm)	6.0
The height of conical louver plate, H_L (cm)	6.0
Conical louver plate number	5.0
The thickness of granular bed sand layer (cm)	2.5
GBF inner diameter (cm)	40.0
Solids mass flow rate, B (g s^{-1})	15.59 ± 0.44 to 20.36 ± 0.68
Injection gas-volumetric flow rate, Q_0 (m^3 s^{-1})	0.0133
Average dust concentration (ppmw)	27,513

various periods, say 1, 2, 3 and 4 h. F is coined as the accumulation weight of attrition fines divided by the initial weight of the collector particles. When the percentage of attrition collector particles (F) versus time approached constant, the operation was at a steady-state. Fig. 5(a) showed the attrition rate reached the steady-state after 3 h. Therefore, all of the experiments data were obtained 4 h after the experiment to be certain of the steady-state in this study.

Moreover, the bigger collector particle size had a higher percentage of attrition fines. Typical changes of the particle size distribution of the initial collector particles (P_0) and the finial collector particles (P_f), is illustrated in Fig. 5(b). In this figure, the change of the average collector particle size was from 795 to 590 μm. The finial particle size of the collector particles became smaller than the initial particle size. This was due to the fact that the collector particles of high velocity transportation resulted in vigorous collision and attrition in the riser. The collector particles in a high gas velocity system are easily split into fines [15].

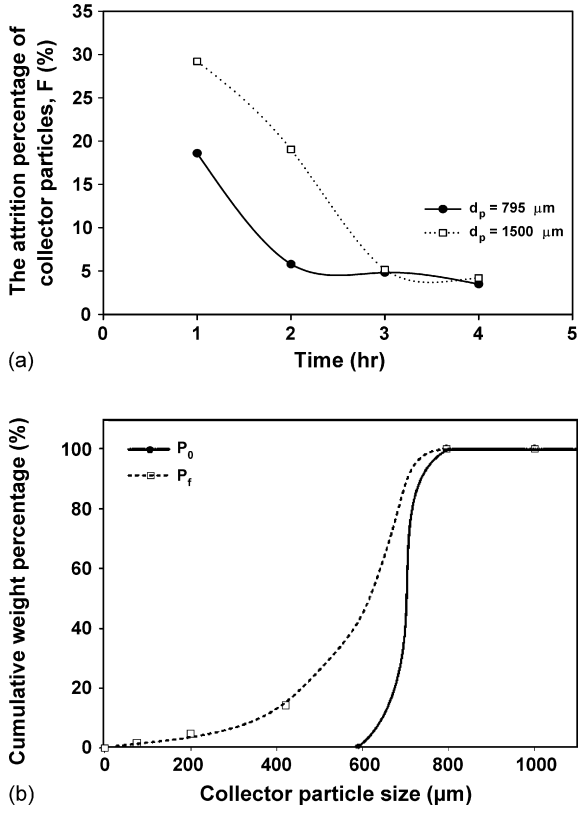

Fig. 5. Attrition and particle size distribution, where (a) the percentage of attrition fines (F) with various periods, (b) the cumulative weight percentage of the initial collector particles (P_0) and the final collector particles (P_f) after 4 h.

3.2. Dust collection efficiency

The dust collection efficiency of different solids mass flow rate (B) with $d_{p0} = 795$ μm and the cyclone type is shown in Fig. 6(a). As the experimental results show, five points of higher dust collection efficiency occurred when the solids mass flow rate was 17.08 ± 0.48 g s^{-1}. Hence, we think that the results make sense. We think that the solids mass flow rate variation from 17.08 ± 0.48 to 20.36 ± 0.67 g s^{-1} was slight. Therefore, the variation of the data of the collection efficiency was small too. Moreover, the effect of the particle size and the separator type were more sensitive than the solids mass flow rate on the collection efficiency. Tardos [16] found that more and more dust

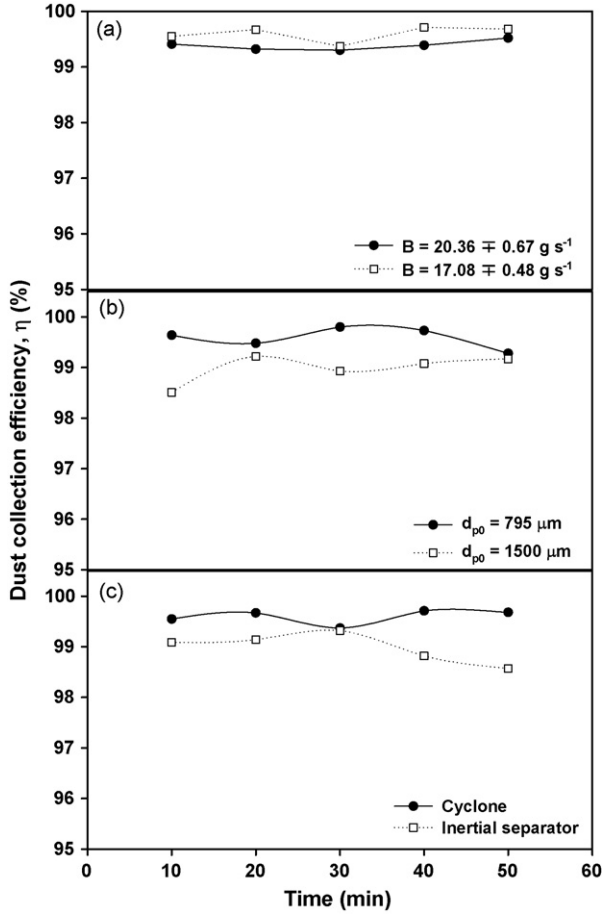

Fig. 6. The dust collection efficiency at different operating times, where (a) the effect of the solid mass flow rate with $d_{p0} = 795$ μm and the cyclone type, (b) the effect of the collector particle size with $B = 15.71 \pm 0.59$ g s^{-1} and the cyclone type (c) the effect of the separator type with $B = 17.08 \pm 0.48$ g s^{-1} and $d_{p0} = 795$ μm.

accumulated and the dust cake formed at the free surface of the GBF. This phenomenon results in a higher filtration efficiency. A faster particle velocity could decrease the dust accumulation at the free surface due to a portion of the surface replaced by the particle that flowed from top-to-bottom of the GBF. It decreased the dust cake at the free surface and thus the dust collection efficiency decreased with an increase in the solids mass flow rate. Therefore, the higher dust collection efficiency occurred when the solids mass flow rate was $17.08 \pm 0.48\,g\,s^{-1}$. These results were similar to that reported by Brown et al. [7] and Henriquez and Macias-Machin [17].

The effect of the collector particle size on dust collection efficiency with $B = 15.71 \pm 0.59\,g\,s^{-1}$ and the cyclone type is shown in Fig. 6(b). Fig. 6(b) illustrates the dust collection efficiency increase while decreasing the collector particle size. This could be due to the dominant effect of smaller collector particles having a larger surface in the GBF. Therefore, the efficiencies of dust impact and interception decreased when the collector particle size increased. This outcome was similar to that reported by Coury et al. [18]. This phenomenon would cause the decrease of dust accumulation at the surface of collector particles. The denser of the moving bed in the GBF results in the dust cake forming easily at the free surface. Therefore, it has a thicker layer of dust accumulating at the free surface of the louver for smaller collector particles. This result is represented by Fig. 7(b). Smaller collector particles had a larger pressure drop. As a result, smaller collector particle size had higher dust collection efficiency than larger ones.

The effect of the separator type in the inlet of GBF on the dust collection efficiency with $B = 17.08 \pm 0.48\,g\,s^{-1}$ and $d_{p0} = 795\,\mu m$ is shown in Fig. 6(c). As shown in this figure, the cyclone type had higher dust collection efficiency compared to the inertial separator type in the inlet of the GBF. This phenomenon resulted in a smaller bed voidage in the GBF with the cyclone type separator than the inertial one. The cut size (d_{100}) of collector particles in the cyclone was 100 μm and most fines of particle size under 100 μm were carried out and the rest of the collector particles were returned to the GBF. These collector particles of fines in the granular bed would cause the bed voidage to be minimal. Geldart [19] found that the extensive particle size distribution is conducive to a smaller bed voidage. The cut size (d_{100}) of the collector particle size in the inertial separator was 300 μm. Therefore, the collector particles in the GBF had a narrower size distribution with the inertial separator than the cyclone one. A narrower size distribution of particles means a bigger bed voidage in the GBF. It resulted in a higher dust collection efficiency with the cyclone type separator.

3.3. Pressure drop

The pressure drop of different solids mass flow rates at different heights of the granular bed filter with $d_{p0} = 795\,\mu m$ and the cyclone type is shown in Fig. 7(a). As shown in this figure, the pressure drop increased when decreasing the solids mass flow rate. The headloss increased with an increase in the relative density of deposits [20]. Similar effects have been observed in the dust collection efficiency section. In addition, the pressure drop increased with an increase in the location height of the GBF (Fig. 7). Due to the location of the dust gas inlet being setup at the top of the GBF, most dust accumulated at the top of the GBF by inertial impaction. As a consequence, the pressure drop increased with a decrease in the solids mass flow rate by increasing the location height of the GBF.

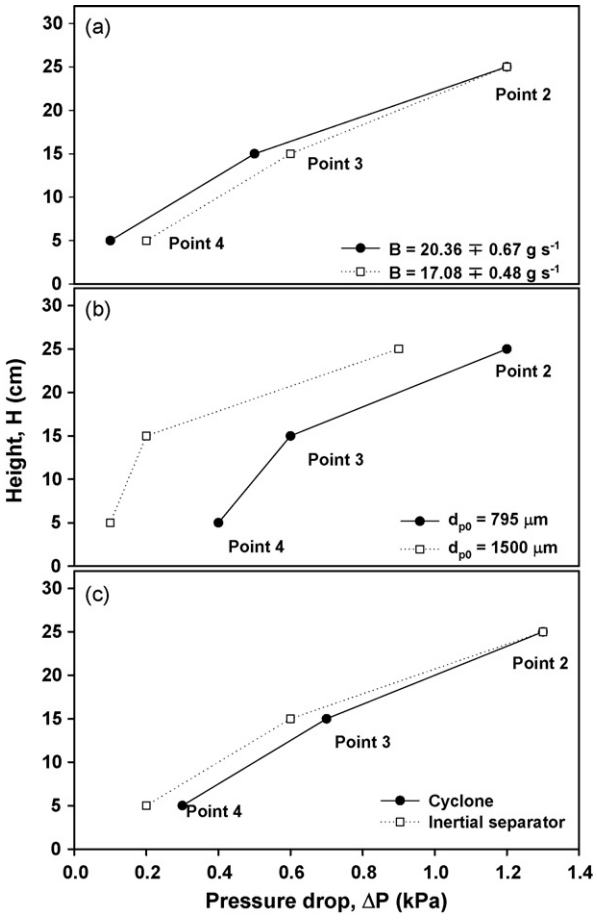

Fig. 7. The pressure drop at different operating times, where (a) the effect of the solid mass flow rate with $d_{p0} = 795\,\mu m$ and the cyclone type, (b) the effect of the collector particle size with $B = 15.71 \pm 0.59\,g\,s^{-1}$ and the cyclone type and (c) the effect of the separator type with $B = 17.08 \pm 0.48\,g\,s^{-1}$ and $d_{p0} = 795\,\mu m$.

The effect of the collector particle size on pressure drop at different location heights in this granular bed filter with $B = 15.71 \pm 0.59\,g\,s^{-1}$ and the cyclone type is shown in Fig. 7(b). The pressure drop increased when decreasing the collector particle size in the GBF. The pressure drop was obviously influenced by different collector particle sizes in the GBF. The collection of dust would cause the bed voidage to become denser by the formation of the dust cake (Fig. 6(b)). As a consequence, the pressure drop increased by decreasing the collector particles in the GBF.

The pressure drop at different gas-solid separator types with $B = 17.08 \pm 0.48\,g\,s^{-1}$ and $d_{p0} = 795\,\mu m$ is shown in Fig. 7(c). As shown in this figure, the cyclone type had higher pressure drop than inertial separator type in the granular bed filter. In light of the cyclone type collecting more attrition fines than the inertial separator in the CGBF-CLPs, the collector particle size distribution was more extensive and the bed voidage became

denser. Therefore, this pressure drop increased simultaneously increasing dust collection efficiency. The increased of pressure drop is linear to the increase of dust collection efficiency.

4. Conclusion

The data of dust collection efficiency and pressure drop was analyzed to provide a better design of the CGBF-CLPs system. It was found that the dust collection efficiency was relative to the effects of the solids mass flow rate, the collector particle size, the separator type and pressure drop.

The increase of dust collection efficiency is linear to the increase of pressure drop. It was found that the highest dust collection efficiency (99.59%) occurred at $B = 17.08 \pm 0.48\ \mathrm{g\ s^{-1}}$, $d_{p0} = 795\ \mu\mathrm{m}$ with the cyclone type. The system of $d_{p0} = 795\ \mu\mathrm{m}$ had higher dust collection efficiency and pressure drop than the one of $d_{p0} = 1500\ \mu\mathrm{m}$. A smaller collector particle size had higher effects of inertial deposition and interception in the GBF. The cyclone type had higher dust collection efficiency and pressure drop because higher amounts of attrition fines were collected and the existence of a denser bed voidage.

Bed voidage and dust cake played important roles in the effects of dust collection efficiency and pressure drop. The dust collection efficiency of the CGBF-CLPs system can be improved by paying attention to the separator, which collects the fines from the attrition of collector particles.

Acknowledgements

This study was supported by The National Science Council of Taiwan, ROC through grant nos. NSC-89-2214-E-035-010 and NSC-92-2214-E-035-002.

References

[1] J.C. Bai, S.Y. Wu, A.S. Lee, Dust collection efficiency analysis in a two-dimensional circulating granular bed filter, J. Air Waste Manage. Assoc. 55 (2006) 684–694.

[2] V. Zakkay, E.A.M. Gbordzoe, A review of hot-gas cleanup devices for PFBC, in: Combustion en Lechos Fluidizados, Program Comett Comunidad Economical European, Zaragoza, Spain, 1989, pp. 216–275.

[3] A.M. Robin, D.Y. Jung, J.S. Kassman, T.F. Leininger, J.K. Wolfenbarger, P.P. Yang, Integration and testing of hot desulfurization and entrained flow gasification for power generation systems, in: R.A. Johnson, S.C. Jain (Eds.), Proceedings of the 12th Annual Gasification and Gas Cleanup Systems Contractors Review Meeting, vol. 1, Hemisphere Publ. Co., Washington, 1992, pp. 713–731.

[4] J.T. Kuo, J. Smid, S.S. Hsiau, C.Y. Wang, C.S. Chou, Stagnant zones in granular moving bed filters for flue gas clean-up, Filtr. Sep. 35 (1998) 529–534.

[5] S.C. Saxena, R.F. Henry, W.F. Podolski, Particulate removal from high temperature, high-pressure combustion gases, Prog. Energ. Combust. 11 (1985) 193–251.

[6] H. Emi, Fundamentals of aerosol filtration, KONA, Party Powder Technol. Jpn. 8 (1990) 83–91.

[7] R.C. Brown, H. Shi, F.G. Clover, S.C. Soo, Similitude study of moving bed granular filter, Powder Technol. 138 (2003) 201–210.

[8] G.I. Tardos, C. Gutfinger, R. Pfeffer, Experiments on aerosol filtration in granular sand beds, J. Colloid. Interf. Sci. 73 (3) (1979) 616–620.

[9] S. Jordan, W. Baumann, W. Lindner, H.R. Paur, Separation of submicron ammonium salt particles from flue gases, Kernforschungszentrum Karisruhe Gmbh, PARTEC, Normberg (F.R.G.), 1989, p. 19.

[10] S. Miyamoto, H.L. Bohn, Filtration of airborne particulates by gravel filters: collection efficiency and pressure drop on filtering fume, J. Air Waste. Mater. 25 (1975) 40–43.

[11] J. Tsubaki, C. Tien, Gas filtration in granular moving beds—an experimental study, Can. J. Chem. Eng. 66 (1988) 271–275.

[12] S. Jordan, W. Linder, Experiences with a cross-flow granular bed filter, Chem. Ing. Tech. 60 (1) (1988) 34–35 (in German).

[13] E. Weingartner, P. Haller, H. Burtscher, U. Baltensperger, Pressure drop across fiber filters, J. Aerosol. Sci. 17 (1996) 639–640.

[14] E. Gal, G. Tardos, R. Pfeffer, A study of inertial effects in granular bed filtration, AIChE J. 31 (1985) 1093–1104.

[15] S.Y. Wu, J. Baeyens, C.Y. Chu, Effect of the grid-velocity on attrition in gas fluidized beds, CJChE 77 (1999) 738–744.

[16] G.I. Tardos, Granular bed filters, in: M.E. Fayed, L. Otten (Eds.), Handbook of Powder Science and Technology, Chapman & Hall, New York, 1997, pp. 771–780.

[17] V. Henriquez, A. Macias-Machin, Hot gas filtration using a moving bed heat exchanger-filter (MHEF), Chem. Eng. Process 369 (1997) 353–361.

[18] J.R. Coury, K.V. Thambimuthu, R. Clift, Capture and rebound of dust in granular bed gas filters, Powder Technol. 50 (1987) 253–265.

[19] D. Geldart, Single particles, fixed and quiescent beds, in: D. Geldart (Ed.), Gas Fluidization Technology, vol. 2, John Wiley, New York, 1986, pp. 11–32 (Chapter 2).

[20] M.A. Boller, M.C. Kavanaugh, Particle characteristics and headloss increase in granular media filtration, Water Res. 29 (4) (1995) 1139–1149.

[21] S.Y. Wu, J. Baeyens, Effect of operated high temperature on minimum fluidization velocity, Powder Technol. 67 (1991) 217–220.

[22] C.Y. Wen, R.F. Hashinger, Elutriation of solid particles from a dense-phase fluidized bed, AIChE. J. 6 (1960) 220–226.